Gazi Üniversitesi
Fen Bilimleri Dergisi
PART C: TASARIM VE TEKNOLOJİ

Gazi University
Journal of Science
PART C: DESIGN AND TECHNOLOGY

GU J Sci, Part C, 14(2): 940-951 (2026)

Comparative Study on the Time-Dependent Electrochemical Corrosion Behavior of Unmodified and Sr-Modified Al-7Si-0.3Mg (A356) Alloys

Gökçe HAPÇI AĞAOĞLU[1*]

[1]*Istanbul University-Cerrahpasa, Faculty of Engineering, Department of Metallurgical and Materials Engineering, Turkey*

Article Info

Research article
Received: 16/04/2026
Revision: 08/06/2026
Accepted: 10/06/2026

Keywords

A356 alloy
Strontium modification
Time-dependent corrosion
Potentiodynamic polarization
EIS

Makale Bilgisi

Araştırma makalesi
Başvuru:16/04/2026
Düzeltme: 08/06/2026
Kabul: 10/06/2026

Anahtar Kelimeler

A356 alaşımı
Stronsiyum modifikasyonu
Zamana bağlı korozyon
Potansiyodinamik polarizasyon
Elektrokimyasal empedans spektroskopisi

Graphical/Tabular Abstract (Grafik Özet)

In this work, the effect of Sr modification on the time-dependent corrosion behavior of A356 alloy was investigated. Sr addition increased the initial electrochemical activity but improved long-term corrosion resistance through the formation of a stable corrosion product layer. / Bu çalışmada, Sr modifikasyonunun A356 alaşımının zamana bağlı korozyon davranışı üzerindeki etkisi incelenmiştir. Sr ilavesi başlangıç elektrokimyasal aktivitesini artırmış, ancak kararlı bir korozyon ürünü tabakası oluşturarak uzun dönem korozyon direncini iyileştirmiştir.

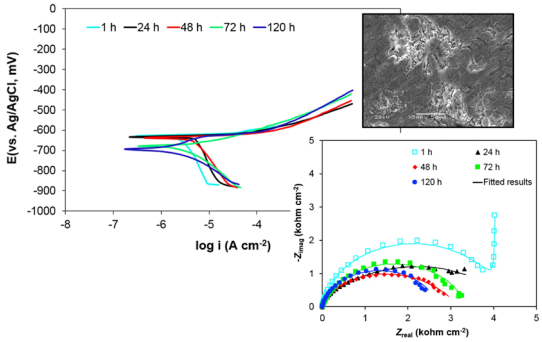

Figure A: *Electrochemical corrosion behavior of Sr-modified A356 alloy and SEM image (120 h) / **Şekil A:** Sr modifiyeli A356 alaşımının elektrokimyasal korozyon davranışı ve SEM görüntüsü (120 saat)*

Highlights (Önemli noktalar)

- *The time-dependent corrosion behavior of unmodified and Sr-modified A356 alloys was investigated. / Modifiye edilmemiş ve Sr modifiyeli A356 alaşımlarının zamana bağlı korozyon davranışı incelenmiştir.*
- *The Sr-modified alloy exhibited approximately 70.3% lower charge transfer resistance after 1 h of immersion. / Sr modifiye alaşım, 1 saatlik daldırma sonrasında yaklaşık %70.3 daha düşük yük transfer direnci göstermiştir.*
- *Sr modification improved the corrosion resistance of the A356 alloy after 120 h of immersion. / Sr modifikasyonu, 120 saatlik daldırma sonrasında A356 alaşımının korozyon direncini iyileştirmiştir.*

Aim (Amaç): *To investigate the effect of 0.02 wt. % Sr modification on the time-dependent electrochemical corrosion behavior of die-cast A356 alloy in a 3.5 wt.% NaCl solution. / %3.5 NaCl çözeltisinde döküm A356 alaşımının zamana bağlı elektrokimyasal korozyon davranışı üzerinde %0.02 Sr modifikasyonunun etkisinin araştırılması amaçlanmıştır.*

Originality (Özgünlük): *The study establishes the relationship between microstructural modification induced by Sr addition and the time-dependent corrosion behavior of A356 alloy through electrochemical analyses and surface characterization. / Çalışma, Sr ilavesiyle oluşan mikroyapısal değişim ile A356 alaşımının zamana bağlı korozyon davranışı arasındaki ilişkiyi elektrokimyasal analizler ve yüzey karakterizasyonu ile ortaya koymaktadır.*

Results (Bulgular): *The unmodified A356 alloy exhibited the lowest corrosion current density (0.050 $\mu A \cdot cm^{-2}$) after 1 h of immersion. Despite its higher initial electrochemical activity, Sr modification improved long-term corrosion resistance through the formation of a stable corrosion product layer. / Modifiye edilmemiş A356 alaşımı, 1 saatlik daldırma sonrasında en düşük korozyon akım yoğunluğunu (0.050 $\mu A \cdot cm^{-2}$) göstermiştir. Sr modifikasyonu, daha yüksek başlangıç elektrokimyasal aktivitesine rağmen, kararlı bir korozyon ürünü tabakası oluşturarak uzun dönem korozyon direncini iyileştirmiştir.*

Conclusion (Sonuç): *Sr modification reduced the initial corrosion resistance but improved the long-term corrosion behavior of the A356 alloy through the formation of a stable protective surface layer. / Sr modifikasyonu başlangıç korozyon direncini azaltmış, ancak kararlı ve koruyucu bir yüzey tabakası oluşturarak A356 alaşımının uzun dönem korozyon davranışını iyileştirmiştir.*

*Corresponding author, e-mail: gokceh@iuc.edu.tr
DOI: 10.29109/gujsc.1931782

GU J Sci, Part C, 14(2): 940-951 (2026)

Gazi Üniversitesi
Fen Bilimleri Dergisi
PART C: TASARIM VE TEKNOLOJİ

Gazi University
Journal of Science
PART C: DESIGN AND TECHNOLOGY

http://dergipark.gov.tr/gujsc

Comparative Study on the Time-Dependent Electrochemical Corrosion Behavior of Unmodified and Sr-Modified Al-7Si-0.3Mg (A356) Alloys

Gökçe HAPÇI AĞAOĞLU[1*]

[1]*Istanbul University-Cerrahpasa, Faculty of Engineering, Department of Metallurgical and Materials Engineering, Turkey*

Article Info

Research article
Received: 16/04/2026
Revision: 08/06/2026
Accepted: 10/06/2026

Keywords

A356 alloy
Strontium modification
Time-dependent corrosion
Potentiodynamic polarization
EIS

Abstract

As-cast Al-Si-Mg alloys are widely used in the production of lightweight components with complex geometries owing to their high corrosion resistance, excellent castability, and improved mechanical properties. This study investigates the influence of strontium (Sr) modification on the time-dependent corrosion behavior of die-cast Al-7Si-0.3Mg (A356) alloy. For this purpose, both unmodified and 0.02 wt.% Sr-modified alloys were systematically examined in a 3.5 wt.% NaCl solution over different immersion times (1, 24, 48, 72 and 120 h). To examine the corrosion behavior of the alloys, electrochemical analyses were carried out employing potentiodynamic polarization and electrochemical impedance spectroscopy (EIS). The results demonstrate that 0.02 wt.% Sr modification increases the initial electrochemical activity of the alloy due to intensified micro-galvanic interactions. Potentiodynamic polarization results indicate that the unmodified alloy exhibits the most favorable corrosion behavior at the initial immersion time (1 h), as evidenced by the lowest corrosion current density (0.050 $\mu A \cdot cm^{-2}$). Consistently, EIS results reveal that the Sr-modified alloy has an approximately 70.3% lower charge transfer resistance (R_{ct}), indicating higher initial electrochemical activity. At longer exposure times, the Sr-modified alloy exhibits enhanced corrosion behavior, due to the formation of a more stable and protective corrosion product layer. Scanning electron microscopy (SEM) analyses of the corroded surfaces revealed that Sr addition promoted a finer and more homogeneous microstructure and facilitated the formation of a more stable corrosion product layer during prolonged immersion. These findings were in good agreement with the electrochemical results and confirmed that, although Sr modification increased the initial electrochemical activity of the A356 alloy, it enhanced the long-term stability of the corrosion product layer.

Modifiye Edilmemiş ve Sr ile Modifiye Edilmiş Al-7Si-0.3Mg (A356) Alaşımlarının Zamana Bağlı Elektrokimyasal Korozyon Davranışının Karşılaştırmalı İncelenmesi

Makale Bilgisi

Araştırma makalesi
Başvuru:16/04/2026
Düzeltme: 08/06/2026
Kabul: 10/06/2026

Anahtar Kelimeler

A356 alaşımı
Stronsiyum modifikasyonu
Zamana bağlı korozyon
Potansiyodinamik polarizasyon
Elektrokimyasal empedans spektroskopisi

Öz

Döküm Al-Si-Mg alaşımları, yüksek korozyon direnci, mükemmel dökülebilirlik ve geliştirilmiş mekanik özellikleri sayesinde karmaşık geometrilere sahip hafif bileşenlerin üretiminde yaygın olarak kullanılmaktadır. Bu çalışmada, stronsiyum (Sr) modifikasyonunun, basınçlı döküm yöntemiyle üretilmiş Al-7Si-0.3Mg (A356) alaşımının zamana bağlı korozyon davranışı üzerindeki etkisi incelenmiştir. Bu amaçla, modifiye edilmemiş ve %0.02 (ağırlıkça) Sr ile modifiye edilmiş alaşımlar, %3.5 NaCl çözeltisi içerisinde farklı daldırma sürelerinde (1, 24, 48, 72 ve 120 saat) sistematik olarak değerlendirilmiştir. Alaşımların korozyon davranışını belirlemek amacıyla, potansiyodinamik polarizasyon ve elektrokimyasal empedans spektroskopisi (EIS) analizleri gerçekleştirilmiştir. Elde edilen sonuçlar, %0.02 Sr modifikasyonunun, mikro-galvanik etkileşimleri artırması nedeniyle başlangıç korozyon hızını modifiye edilmemiş A356 alaşımına kıyasla yükselttiğini göstermektedir. Potansiyodinamik polarizasyon sonuçları, modifiye edilmemiş alaşımın başlangıç daldırma süresinde (1 saat) en düşük korozyon akım yoğunluğu (0.050 $\mu A \cdot cm^{-2}$) ile en iyi korozyon performansını sergilediğini ortaya koymuştur. Bununla uyumlu olarak, EIS sonuçları Sr ile modifiye edilmiş alaşımın yaklaşık %70.3 daha düşük yük transfer direnci (R_{ct}) değerine sahip olduğunu ve bunun daha yüksek başlangıç elektrokimyasal aktiviteye işaret ettiğini göstermektedir. Bununla birlikte, daha uzun daldırma sürelerinde Sr ile modifiye edilmiş alaşımın, daha kararlı ve koruyucu bir korozyon ürünü tabakasının oluşumu sayesinde gelişmiş korozyon direnci sergilediği belirlenmiştir. Korozyona uğramış yüzeylere ait taramalı elektron mikroskobu (SEM) analizleri, Sr ilavesinin daha ince ve homojen bir mikroyapı oluşumunu teşvik ettiğini ve uzun süreli daldırma koşullarında daha kararlı bir korozyon ürün tabakasının gelişimini desteklediğini göstermiştir. Elde edilen bulgular elektrokimyasal sonuçlarla uyumlu olup, Sr modifikasyonunun A356 alaşımının başlangıçtaki elektrokimyasal aktivitesini artırmasına karşın, korozyon ürün tabakasının uzun süreli kararlılığını artırdığını doğrulamaktadır.

*Corresponding author, e-mail: gokceh@iuc.edu.tr
DOI: 10.29109/gujsc.1931782

1. INTRODUCTION (GİRİŞ)

Aluminium-silicon (Al-Si) casting alloys have become key materials in automotive, aerospace, and engineering applications due to their low density, high strength-to-weight ratio, and excellent castability, and favorable mechanical and corrosion properties under appropriate processing conditions [1-2]. Al-Si cast alloys account for approximately 80-90% of global Al castings production [1]. Among hypoeutectic Al-Si alloys, the 356 series Al alloys are considered one of the most widely used materials within the Al-Si-Mg alloy systems. The corrosion performance of Al-Si-Mg casting alloys is also of critical importance for their industrial applications. Corrosive agents encountered during manufacturing, service, and maintenance processes pose significant challenges to the structural integrity of components, particularly those produced from Al alloys. Corrosion-induced damage may lead to costly repairs and component replacements while adversely affecting operational efficiency and safety. Therefore, understanding the corrosion performance of Al-Si-Mg alloys, as well as the factors governing the increase or decrease in corrosion resistance and the underlying corrosion mechanisms, is of great importance for improving the reliability and durability of these alloys in industrial applications [3-8]. Corrosion characteristics in Al-Si alloys are primarily governed by the physicochemical properties, volume fraction, and morphological features of the primary phases (primary α-Al and eutectic silicon), along with the presence and distribution of secondary intermetallic phases (e.g., AlFeSi, AlFeSiMn, Mg_2Si, and AlFeSiMg) [8,9]. In Al-Si casting alloys, the unmodified eutectic Si typically exhibits a plate-like morphology within the aluminum matrix. Because the solubility of silicon in aluminum is very limited, silicon tends to precipitate as coarse flake-like particles of nearly pure silicon. Such heterogeneous distribution of silicon phases results in non-uniform mechanical and electrochemical properties within the alloy [2,10-12]. Several studies have reported that the morphology and distribution of eutectic silicon play a critical role in determining the corrosion behavior of Al-Si alloys. Tahamtan et al. [13] demonstrated that coarse Si particles in A356 alloys promote the formation of a less protective oxide film in aqueous environments. Similarly, Pardo et al. [14] reported that exposure of A360 alloy to NaCl solutions promotes the formation of a porous $Al_2O_3 \cdot H_2O$ corrosion film, which initially acts as a protective barrier but may crack over time, allowing chloride ions to penetrate the surface. Furthermore, Olohunde et al. [15] reported that during immersion corrosion of hypoeutectic Al-Si alloys in NaCl solution, the corrosion current density decreased with increasing immersion time. This behavior can be explained by the development of a compact corrosion product layer on the metal surface, which limits the interaction between the metal and the surrounding corrosive environment.

In this context, modification treatments are widely applied to molten Al-Si alloys to refine eutectic silicon morphology and control the distribution of secondary and intermetallic phases. These microstructural changes significantly influence corrosion behavior by affecting the composition and stability of the surface oxide layer. Consequently, the integrity of the passive film and overall corrosion performance are closely linked to these microstructural features [2,12,16-18]. Among the various modifier elements, strontium (Sr) is one of the most widely used in aluminum casting to modify melt characteristics. The incorporation of Sr has been reported to modify the eutectic Si phase, transforming its coarse plate-like structure into a fine fibrous morphology [2,18]. In aluminum alloys, the passive layer is typically composed of an amorphous aluminum oxide film, and Sr modification may affect resistance to chloride-induced pitting corrosion by modifying the characteristics and stability of this passive film [19,20]. However, there is still no clear consensus in the literature regarding the effect of Sr modification on the corrosion behavior of Al-Si alloys. Lee et al. [20] examined the influence of Sr addition on the corrosion characteristics of A356 alloy in a 3.5 wt.% NaCl solution. The incorporation of Sr resulted in a shift of the corrosion potential (E_{corr}) from -695 mV to -883 mV, accompanied by an increase in corrosion current density (i_{corr}) from 0.59 to 1.86 $\mu A \cdot cm^{-2}$. This microstructural modification refined eutectic Si particles within the eutectic regions, thereby increasing the α-Al/Si interfacial area and enhancing galvanic coupling. These interfaces are considered the most susceptible sites for galvanic corrosion, leading to increased electrochemical activity and promoting the initiation of localized pitting in the interdendritic α-Al phase. Similarly, Lian et al. [21] reported that the unmodified Al-7Si alloy exhibited superior corrosion performance compared with Sr- and/or Sc-containing alloys. The higher corrosion current observed in the modified alloys was associated with the increased α-Al/eutectic Si interfacial area. Consistent with these findings, Liao et al. [22] also reported that the highest corrosion resistance was observed in the unmodified Al-11.7 wt.%Si alloy based on salt spray tests performed in a 5 wt.% NaCl aqueous solution. After 120 hours of salt spray

corrosion testing, corrosion-related cracking developed on the surface of the Sr-modified alloy. According to Farahany et al. [23], the presence of 400 ppm Sr promotes a more negative corrosion potential and higher corrosion activity due to the expansion of interfacial regions between primary Al and eutectic Si phases. Likewise, Osório et al. [11] observed that modification of Al-9 wt.%Si alloys results in reduced corrosion performance, associated with an increase in α-Al/Si interfacial regions. Duygun et al. [24] demonstrated that modification with Sr in AlSi9 alloy produced finer eutectic phases and more equiaxed dendrites; however, the corrosion behavior varied depending on the Sr content. They observed that the incorporation of 200 ppm Sr increased the eutectic phase area from 26.1% to 33.0% and increased the corrosion rate in a 3.5 wt.% NaCl solution due to enhanced galvanic interactions. Moreover, the corrosion resistance of the AlSi9 alloy was found to deteriorate with increasing immersion time. In contrast, Öztürk et al. [25] reported improved corrosion performance in die-cast A356 alloy containing 120 ppm Sr during short-term immersion, which was attributed to the formation of a more stable surface oxide film.

In this study, the corrosion behavior of unmodified and 0.02 wt.% Sr-modified Al-7Si-0.3Mg (A356) alloys at immersion times of 1, 24, 48, 72, and 120 h in a 3.5 wt.% NaCl solution was systematically investigated. Corrosion performance was evaluated using potentiodynamic polarization measurements combined with electrochemical impedance spectroscopy (EIS). Furthermore, SEM observations were conducted to assess the evolution of corrosion morphology with immersion time. Accordingly, the combined effects of Sr modification and immersion time on the corrosion mechanisms of Al-Si-Mg alloys were elucidated.

2.MATERIALS AND METHODS (MATERYAL VE METOD)

Commercially supplied Al-7Si-0.3Mg (A356) ingots were cut into smaller segments, dried, and remelted to produce both unmodified and Sr-modified A356 alloys. Melting was performed in a SiC crucible using an electrically heated, atmosphere-controlled resistance furnace, and the temperature was maintained at 750 °C throughout the process. The chemical modification was performed by the addition of an Al15Sr master alloy into the molten aluminum. The alloys were cast into die mold in cylindrical samples of dimensions Ø15 X 150 mm. The cast parts were prepared to the required dimensions prior to corrosion testing. In this study, A356-base refers to the unmodified Al-7Si-0.3Mg alloy, whereas A356-Sr denotes the alloy modified with approximately 200 ppm Sr. After casting, the samples were sectioned, prepared metallographically, and examined by optical microscopy to characterize the as-cast microstructure.

The corrosion-related electrochemical behavior of cast Al-7Si-0.3Mg alloys was systematically investigated using a Gamry Reference 600 instrument. A standard three-electrode system was utilized for all experiments conducted in a 3.5 wt.% NaCl electrolyte (25 °C, pH 6.5) prepared from analytical-grade reagents and deionized water. Die-cast A356-base and A356-Sr alloys served as working electrodes, with an exposed surface area of 1 cm² in the corrosive medium. A platinum sheet was utilized as the auxiliary electrode, whereas a saturated Ag/AgCl electrode functioned as the reference. The specimens acting as working electrodes were maintained in the electrolyte for predetermined durations of 1, 24, 48, 72, and 120 h prior to electrochemical evaluation. EIS spectra were recorded prior to potentiodynamic polarization tests over a frequency range of 100 kHz to 0.1 Hz using a 5 mV sinusoidal perturbation at the open circuit potential (E_{OCP}). Then, appropriate electrochemical equivalent circuit (EEC) models that best fit the experimental results were selected and analyzed using Gamry Echem Analyst software (EIS 300). After reaching a stable E_{OCP}, potentiodynamic polarization tests was performed by scanning the potential from -0.2 V to +1.5 V vs E_{OCP} at a rate of 1 mV s^{-1} to obtain polarization responses. Tafel extrapolation of the polarization data was employed to determine corrosion parameters, including corrosion potential (E_{corr}) and corrosion current density (i_{corr}). All measurements were performed in triplicate under identical conditions to confirm reproducibility, and the corresponding statistical errors are presented in the tables. After the electrochemical tests, the corroded surfaces of the A356-base and A356-Sr alloys were characterized by scanning electron microscopy (SEM, JEOL JSM 5600) to evaluate immersion-time-dependent changes in corrosion morphology.

3.RESULTS (BULGULAR)

The microstructures of the die-cast A356-base and the A356-Sr alloys are shown in Fig. 1. As observed in Fig. 1a, the unmodified A356 alloy exhibits a microstructure consisting of an Al-rich dendritic matrix (α-Al phase) and an interdendritic eutectic constituent. The eutectic structure is characterized by coarse and plate-like Si particles distributed

within the Al-rich matrix. With the addition of 0.02 wt.% Sr, a pronounced change in the eutectic Si morphology is evident. As shown in Fig. 1b, the coarse plate-like Si particles are replaced by a refined and more uniformly distributed eutectic Si structure, resulting in a more homogeneous microstructure. This microstructural refinement increases the α-Al/Si interfacial area and modifies the micro-galvanic interactions within the alloy, which are known to influence its corrosion behavior.

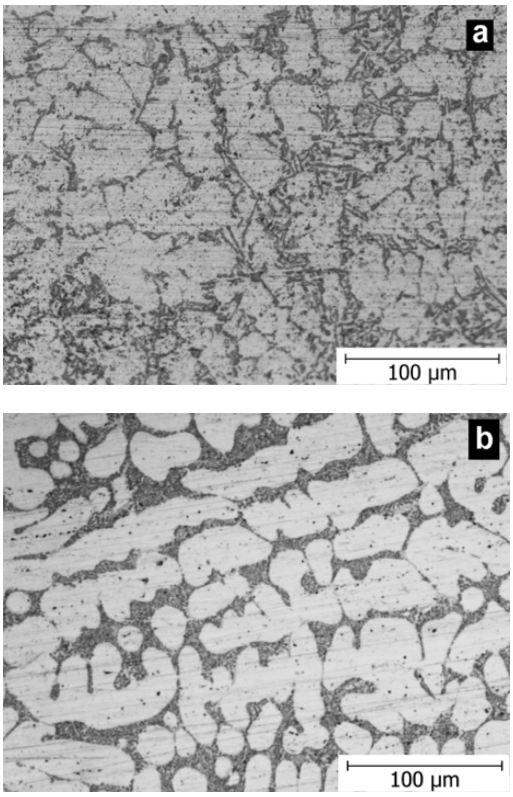

Figure 1. Microstructure images of (a) A356-base and (b)A356-Sr alloys (A356-base (a) ve A356-Sr (b) alaşımlarının mikroyapı görüntüleri)

Potentiodynamic polarization curves of the A356-base and A356-Sr aluminum alloys after exposure to 3.5 wt.% NaCl solution for 1, 24, 48, 72, and 120 h are presented in Figs. 2 and 3. Key corrosion parameters, including i_{corr} and E_{corr} were calculated from the polarization data through Tafel analysis, with the corresponding results compiled in Table 1.

For the A356-base alloy, a clear time-dependent corrosion behavior is observed in Fig. 2. After 1 h of immersion, the alloy exhibits the lowest i_{corr} value (0.050 $\mu A \cdot cm^{-2}$), indicating superior corrosion resistance at the initial stage. This phenomenon is associated with the presence of a dense and stable native Al_2O_3 film, which provides effective passivation and acts as a barrier against chloride ion attack. The polarization curve shows a sharp increase in current density at approximately -700 mV, which can be associated with the pitting potential (E_{pitt}). At this early exposure stage, the alloy demonstrates passivation behavior attributed to the presence of a dense and stable native Al_2O_3 film acting as an effective barrier against Cl^- attack. The polarization curve shows a sharp increase in current density at approximately -700 mV, the E_{pitt} value, suggesting the onset of localized breakdown of the passive film. With increasing immersion time to 24 and 48 h, i_{corr} values increase significantly, indicating accelerated corrosion kinetics. This can be associated with the progressive degradation of the passive oxide film in the aggressive chloride-containing environment. Chloride ions are known to penetrate and destabilize the passive layer, promoting localized dissolution of the aluminum matrix [24-27]. At 72 h, a decrease in i_{corr} is observed, suggesting the formation of a partially protective corrosion product layer. This layer is likely composed of aluminum hydroxide and/or oxyhydroxide species, which temporarily reduce ionic transport and hinder further dissolution. However, upon prolonged immersion (120 h), i_{corr} increases again, indicating the instability and breakdown of this corrosion product layer under continued chloride exposure, leading to renewed corrosion activity. The evolution of E_{corr} values further supports these observations. The positive shift in E_{corr} up to 24 h indicates a relative stabilization of the alloy surface, which can be attributed to the formation of corrosion products layer. However, the simultaneous increase in i_{corr} suggests that this surface layer is not fully protective and may be unstable in the chloride-containing environment. After 24 h of immersion, E_{corr} values exhibit minor fluctuations, reflecting a dynamic balance between metastable pitting events and repassivation processes. This behavior is characteristic of aluminum alloys in chloride media, where continuous breakdown and reformation of the passive film occur. Furthermore, the anodic branch of the polarization curves at longer immersion times suggests the formation and partial breakdown of surface films, confirming the unstable nature of the corrosion product layer [26-30].

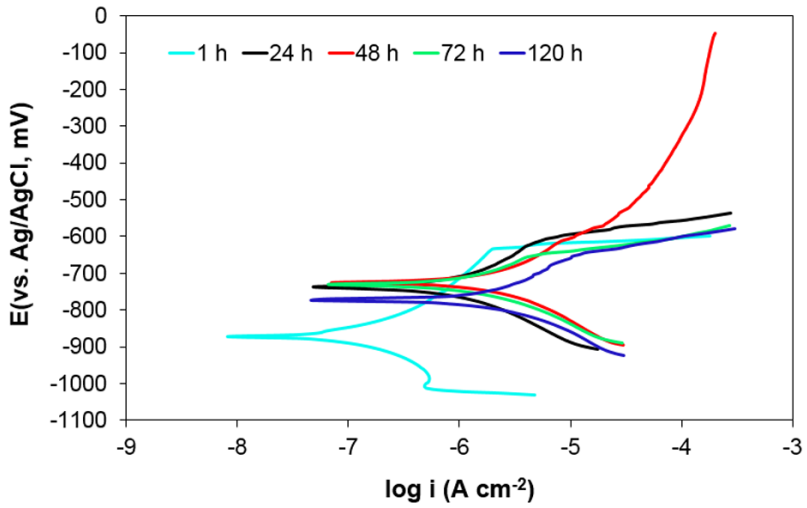

Figure 2. Potentiodynamic polarization behavior of the A356-base alloy as a function of immersion time
(A356-base alaşımının daldırma süresine bağlı potansiyodinamik polarizasyon davranışı)

It is well established that the corrosion behavior of A356 alloy is strongly influenced by the presence of eutectic silicon. Silicon has a more noble electrochemical potential than aluminum; therefore, in chloride environments, the α-Al matrix acts anodically relative to the Si phase, leading to preferential dissolution of aluminum. This micro-galvanic coupling is particularly pronounced at the interfaces between the α-Al matrix and eutectic Si particles. In the case of the unmodified alloy, the coarse plate-like eutectic Si morphology (see Fig. 1a) promotes localized disruption of the passive film and inhibits the formation of a uniform and protective oxide layer, thereby facilitating localized corrosion initiation at these interfacial regions. In addition, the cathodic oxygen reduction reaction is preferentially supported on Si-rich regions, further accelerating anodic dissolution of the surrounding aluminum matrix [3,5,12,14,10].

The potentiodynamic polarization curves of the Sr-modified A356 alloy obtained at different immersion times are presented in Fig. 3. Compared with the unmodified A356 alloy, the Sr-modified alloy exhibits consistently higher i_{corr} values at all immersion times, indicating lower corrosion resistance, as also summarized in Table 1. This behavior can be attributed to the modification of eutectic Si morphology from coarse plate-like structures to fine fibrous particles induced by Sr addition (see Fig. 1b). This refinement significantly increases the number density of Si particles and, consequently, the total interfacial area between the α-Al matrix and the Si phase. As a result, micro-galvanic interactions are intensified, accelerating localized corrosion processes [2,17,19-21]. It should also be noted that the corrosion behavior of A356-Sr alloys may be additionally influenced by casting-related factors such as porosity and intermetallic phase distribution, which can further contribute to localized corrosion susceptibility [3,18]. The i_{corr} value increases from 1.72 to 5.13 $\mu A \cdot cm^{-2}$ between 1 h and 24 h of immersion, reflecting an intensified corrosion process at early exposure stages. However, with prolonged immersion (24-120 h), a noticeable decrease in i_{corr} is observed for the A356-Sr alloy. The polarization curves exhibit a clear tendency toward passivation at longer exposure times, indicating the gradual formation of a more stable and protective corrosion product layer on the surface. This suggests that although the initial corrosion rate is higher due to intensified micro-galvanic interactions, the refined microstructure may facilitate the development of a more homogeneous corrosion product layer over time. The E_{corr} values of the Sr-modified alloy at all immersion times are shifted toward more positive potentials compared to the unmodified alloy. The E_{corr} values remain relatively stable up to 48 h, followed by a slight decrease at longer immersion times. This trend suggests that Sr affects surface electrochemical reactions and facilitates the gradual formation of a more stable and protective surface layer under prolonged exposure conditions.

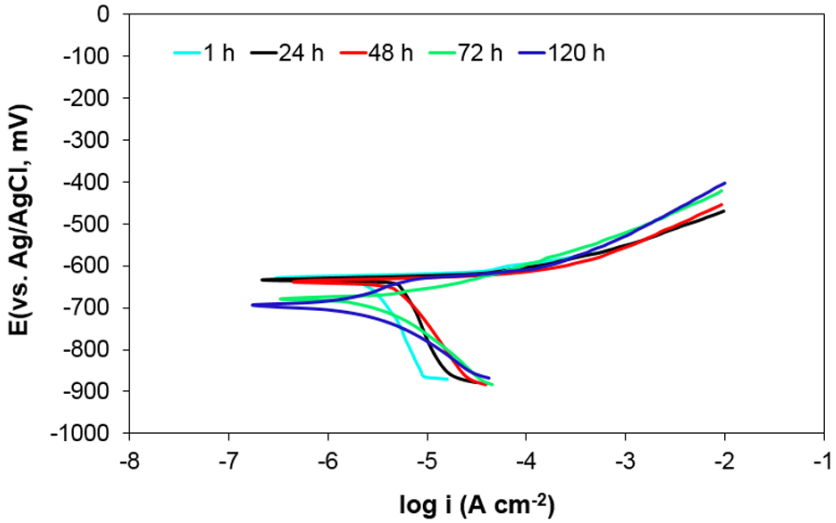

Figure 3. Potentiodynamic polarization behavior of the A356-Sr alloy as a function of immersion time (A356-Sr alaşımının daldırma süresine bağlı potansiyodinamik polarizasyon davranışı)

Table 1. Electrochemical parameters of A356-base and A356-Sr alloys determined by potentiodynamic polarization tests (Potansiyodinamik polarizasyon deneyleri sonucunda elde edilen A356-base ve A356-Sr alaşımlarının elektrokimyasal parametreleri)

	Immersion Time (h)	$-E_{corr}$ (mV)	i_{corr} (µA cm^{-2})
A356-base			
	1	873±5	0.05±0.07
	24	736±4	0.51±0.21
	48	727±2	0.75±0.20
	72	731±2	0.64±0.10
	120	775±5	0.75±0.11
A356-Sr			
	1	630±2	1.72±0.23
	24	635±1	5.13±0.32
	48	638±3	4.30±0.12
	72	680±4	2.60±0.11
	120	694±4	1.01±0.08

Fig. 4 (a and b) show the Nyquist plots of the A356-base and A356-Sr alloys, respectively, obtained at increasing immersion times. The solid lines in the Nyquist plots represent the fitted curves. The Nyquist curves were fitted using two-time constant electrochemical equivalent circuit (EEC) models, as shown in Fig. 5 (a and b). In Fig. 4a, the impedance spectra of the unmodified A356 alloy exhibit a capacitive behavior at all immersion times, along with a diagonal line in the low-frequency region. This behavior indicates that both charge-transfer reactions and diffusion processes occur simultaneously in the unmodified alloy throughout the immersion period. In contrast, for the Sr-modified A356 alloy (Fig. 4b), this feature is observed only after 1 h of immersion, and its disappearance at longer exposure times suggests a suppression of diffusion-controlled processes. This behavior can be attributed to the formation of a more stable and protective corrosion product layer in the presence of Sr, which limits ionic transport at the alloy/electrolyte interface [9,16,24,25,29]. For both alloys, the largest capacitive loop diameter is observed after 1 h of immersion, corresponding to the highest charge-transfer resistance and lowest corrosion rate. With increasing immersion time, the loop diameter decreases, indicating progressive degradation of corrosion resistance. Since the capacitive loop diameter is directly related to the charge-transfer resistance, larger diameters correspond to improved corrosion resistance [24,25,29]. For the unmodified alloy, the smallest capacitive loop diameter is observed after 48 h followed by a slight increase at longer immersion

times. This behavior suggests an initial breakdown of the native oxide film, followed by partial recovery due to the formation of corrosion product layers such as $Al(OH)_3/Al_2O_3$ on the surface. The Sr-modified alloy exhibits smaller loop diameters at 1 h compared to the unmodified alloy, consistent with polarization results. However, the decrease in loop diameter with immersion time was less pronounced for the Sr-modified alloys, indicating a more effective barrier effect at the alloy/electrolyte interface. This behavior suggests that Sr modification retards the progressive degradation of the electrochemical response during prolonged exposure.

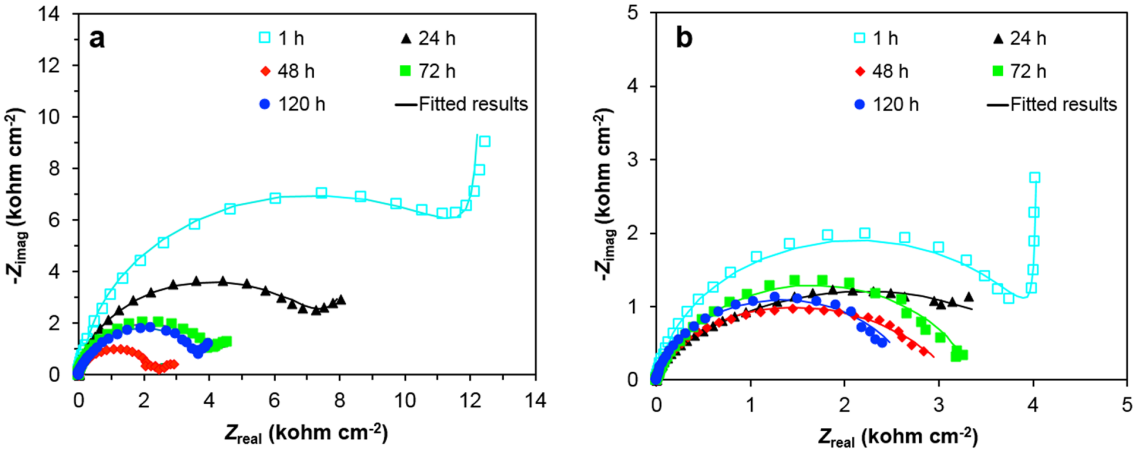

Figure 4. Nyquist diagrams of A356-base (a) and A356-Sr (b) alloys at different immersion times (A356-base (a) ve A356-Sr (b) alaşımlarının farklı daldırma sürelerindeki Nyquist diyagramları).

For the unmodified A356 alloy, the EEC model shown in Fig. 5a was employed for all immersion times. In contrast, for the Sr-modified alloy, the EEC model in Fig. 5a was used to interpret the Nyquist diagram obtained after 1 h of immersion, whereas the EEC model presented in Fig. 5b was applied for the other immersion times.

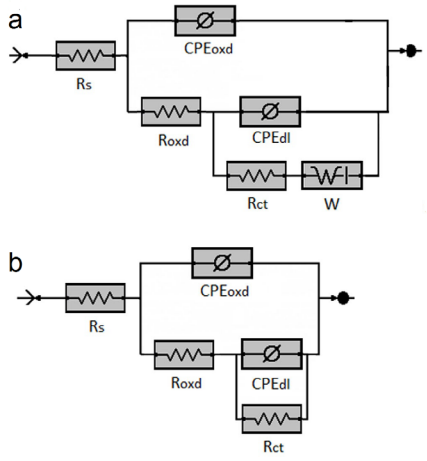

Figure 5. EEC models employed to fit the EIS responses of A356-base and A356-Sr alloys (A356-base ve A356-Sr alaşımlarının EIS yanıtlarının modellenmesinde kullanılan EEC modelleri)

In the EEC models, R_s value correspond to the uncompensated electrolyte resistance, reflecting the ionic resistance of the bulk solution between the working and reference electrodes. The R_{oxd}-CPE_{oxd} element pair characterizes the electrochemical behavior of the oxide film formed on the A356 alloy surface. The R_{ct}-CPE_{dl} pair reflects the interfacial charge transfer kinetics associated with the corrosion process. The R_{ct} parameter represents the resistance to interfacial electron transfer and is inversely correlated with the corrosion rate. The formation of an electrical double layer at the electrode/electrolyte interface suggests that the corrosion process is primarily governed by charge transfer kinetics [6,19,30]. The circuit elements denoted as constant phase elements (CPE_{oxd} and CPE_{dl}) represent the non-ideal capacitive behavior associated with the respective resistive components. A CPE was used instead of an ideal capacitor in the EEC model due to surface heterogeneity; this behavior is associated with deviations from ideal capacitive response at the interface. The CPE elements are defined by the Y_0 and n parameters. The presence of a straight line at low frequencies in the Nyquist plots indicates Warburg impedance, associated with Cl^- ion diffusion toward the alloy surface. This element reflects the diffusion-controlled processes contributing to the overall corrosion mechanism. Ion diffusion through the surface layer and the capacitive response of the oxide film can be interpreted using the Warburg parameter. An increase in B accompanied by a decrease in Y_0 indicates slower diffusion kinetics within the surface layer. The time-dependent variation of these parameters correlates well with the corrosion resistance behavior [9,24,29]

Table 2. Electrochemical parameters of A356-base and A356-Sr alloys obtained from EIS fitting results
(EIS fit sonuçlarından elde edilen A356-base ve A356-Sr alaşımlarına ait elektrokimyasal parametreler)

	R_{oxd} (Ωcm^2)	CPE_{oxd} ($\mu\Omega^{-1}cm^{-2}s^n$)	n	R_{ct} ($k\Omega cm^2$)	CPE_{dl} ($\mu\Omega^{-1}cm^{-2}s^n$)	n	Y_0 ($m\Omega^{-1}cm^{-2}s^{1/2}$)	B ($s^{1/2}$)
A356-base								
1h	184.2±12	46.1±4	0.98	13.8±0.1	12.4±3	0.99	10.1±5	0.18±0.1
24h	32.5±4	64.5±2	0.99	7.9±0.1	18.6±2	0.99	22.0±4	0.12±0.2
48h	20.5±5	82.2±1	0.89	2.1±0.4	25.8±1	0.87	20.0±2	0.10±0.2
72h	91.7±3	56.0±3	0.94	4.1±0.3	17.2±3	0.92	18.3±2	0.12±0.1
120h	81.1±3	57.0±3	0.99	3.8±0.2	21.4±1	0.96	17.1±3	0.11±0.3
A356-Sr								
1h	154.0±1	52.1±5	0.96	4.1±0.2	29.9±6	0.92	12.9±2	0.05±0.03
24h	98.8±1	76.2±3	0.88	3.5±0.3	91.9±4	0.96	-	-
48h	87.4±1	77.1±3	0.88	3.0±0.1	60.0±4	0.96	-	-
72h	88.1±1	72.0±1	0.99	3.3±0.1	36.7±7	0.95	-	-
120h	78.2±1	81.2±1	0.98	2.7±0.4	21.9±3	0.98	-	-

In the A356-base alloy, the high R_{ct} value (13.8 $k\Omega \cdot cm^2$) and low CPE_{dl} value (12.4 $\mu\Omega^{-1} \cdot cm^{-2} \cdot s^n$) obtained after 1 h of immersion demonstrate the enhanced corrosion resistance of the alloy. High R_{oxd} and low CPE_{oxd} values indicate superior corrosion resistance of the protective surface film. After 1 h of immersion, the results suggest a smaller effective contact area between the electrolyte and the aluminum surface. With increasing exposure time, the oxide layer was found to deteriorate progressively. The highest B and the lowest Y_0 values were obtained after 1 h of immersion (see Table 2), indicating that the diffusion of Cl^- ions through the alloy surface was more restricted at this stage. The gradual decrease in B values up to 48 h corresponds to the progressive breakdown of the oxide/hydroxide layer. After 1 h of immersion, the R_{ct} value of the Sr-modified alloy (A356-Sr) was found to be approximately 70.3% lower than that of the unmodified alloy (A356-base), indicating a more active electrochemical behavior at the initial stage. This can be attributed to the altered microstructural features induced by Sr, which promote anodic dissolution. However, with increasing immersion time, the reduction in R_{ct} values becomes less pronounced compared to the unmodified alloy, suggesting the development of a more stable and protective corrosion product layer [19,24,30]. Consistent trends observed in the other impedance parameters (R_{oxd}, Y_0, and B) further support the limited presence of Cl^- ions at 1 h and their relatively enhanced diffusion in the presence of Sr. The disappearance of Y_0 and B parameters at longer exposure time indicates a transition from diffusion-controlled processes to charge-transfer-controlled corrosion behavior, which is associated with the formation of a surface barrier limiting Cl^- ion transport. In this context, the Sr-modified alloy exhibits a more stable interfacial response, despite its initially lower corrosion resistance. As expected, R_{ct} values decrease with prolonged exposure due to progressive surface layer degradation and increased electrolyte penetration. However, this decrease is less pronounced in the Sr-modified alloy, suggesting that it maintains a relatively more resistant interface against Cl^- ion ingress. A similar trend is observed for the R_{ox} values, which decrease with immersion time but remain comparatively more stable in the presence of Sr, confirming its stabilizing effect on the corrosion product layer. These findings demonstrate that Sr addition not only influences the early-stage electrochemical response but also contributes to improved interfacial stability under extended exposure conditions. Regardless of Sr content, the corrosion rate increases with prolonged immersion time due to progressive surface degradation and corrosion product formation [24,29]. A general decline in both R_{oxd} and R_{ct} values is observed with exposure time; however, this decrease is less pronounced in the presence of Sr, indicating that the surface maintains its protective characteristics more effectively during prolonged exposure [19]. These corrosion products act as a semi stable barrier, limiting localized pit propagation and retarding Cl^- ion penetration into the alloy surface. Overall, these results demonstrate that Sr addition leads to a dual effect: while it promotes higher initial reactivity, it significantly enhances the stability of the corrosion product layer at longer exposure times, thereby mitigating localized corrosion and limiting the penetration of aggressive ions.

The SEM micrographs of the corroded surfaces obtained after 1 h and 120 h of immersion are shown in Fig. 6. As shown in Figs. 6a and b, the corroded surfaces of the A356-base alloy after 1 h and 120 h of immersion exhibited coarse, plate-like silicon particles. As mentioned above, the dissolution of the α-Al dendrites resulted in an irregular and needle-like morphology consisting predominantly of the remaining Al-Si eutectic structure. The relatively high corrosion resistance at the early stage of exposure (1 h) is attributed to the combined effect of the native oxide layer and the coarse Si morphology, which minimizes micro-galvanic activity within the alloy microstructure (Fig. 6a). Corrosion was found to occur predominantly around Si particles located in the eutectic regions. Since the Si phase possesses a nobler electrochemical potential than the eutectic Al phase, the primary α-Al matrix becomes anodically active and preferentially dissolves in the aggressive chloride containing environment [25]. After 120 h of immersion, the lower corrosion resistance exhibited by the unmodified A356 alloy can be attributed to the irregular, needle-like, and coarse Si particles (Fig. 6b), which hinder the formation and stability of a continuous and protective oxide film. These weak points within the oxide film serve as preferential sites for corrosion initiation, thereby promoting the propagation of localized corrosion [24,25].

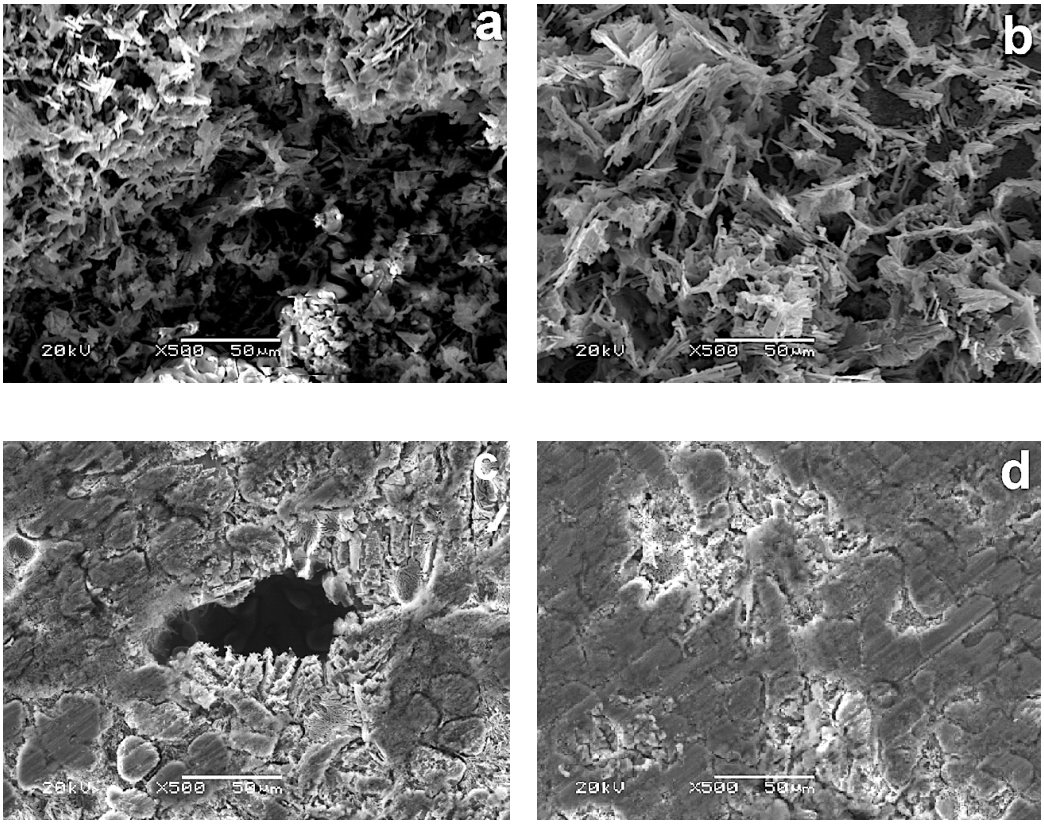

Figure 6. SEM micrographs of the corroded surfaces of A356-base ((a) 1 h and (b) 120 h) and A356-Sr ((c) 1 h and (d) 120 h) alloys after immersion in 3.5 wt.% NaCl solution (%3,5 NaCl çözeltisinde daldırma sonrasında A356-base ((a) 1 saat ve (b) 120 saat) ve A356-Sr ((c) 1 saat ve (d) 120 saat) alaşımlarının korozyona uğramış yüzeylerine ait SEM görüntüleri)

As shown in Figs. 6c and d, the α-Al dendrites in the Sr-modified A356 alloy were not completely dissolved after 1 h and 120 h of immersion. Moreover, the coarse, plate-like morphology characteristic of the unmodified alloy was not observed. The addition of Sr resulted in a finer and more homogeneous eutectic Si morphology. Although pitting corrosion was observed in some interdendritic regions of the Sr-modified A356 alloy, the primary α-Al phase and the dendritic structure were largely preserved. The refinement and homogenization of eutectic Si particles induced by Sr addition appear to enhance the stability and protective character of the oxide film during prolonged immersion, thereby significantly reducing the dissolution of α-Al dendrites. The finer microstructure formed in the presence of Sr and the preservation of the eutectic phase morphology significantly reduced the dissolution of α-Al dendrites. Furthermore, the formation of a

more stable and protective surface film improved resistance against Cl^- ion penetration and reduced localized corrosion during prolonged immersion [24,25]. The immersion-time-dependent morphological changes observed in the A356-base and A356-Sr alloys were consistent with the results obtained from the electrochemical analyses.

4.CONCLUSIONS (SONUÇLAR)

The electrochemical corrosion behavior of unmodified and 0.02 wt.% Sr-modified Al-7Si-0.3Mg (A356) alloys in 3.5 wt.% NaCl solution was evaluated during immersion periods of 1, 24, 48, 72, and 120 h. The unmodified A356 alloy exhibited higher initial corrosion resistance, as evidenced by the lowest i_{corr} value of 0.050 $\mu A \cdot cm^{-2}$ after 1 h of immersion. In contrast, the Sr-modified alloy showed higher initial corrosion activity, with i_{corr} increasing from 1.72 to 5.13 $\mu A \cdot cm^{-2}$ between 1 and 24 h. However, during prolonged immersion (24-120 h), the gradual decrease in i_{corr} indicated the formation of a more stable and protective corrosion product layer, leading to improved corrosion resistance. The EIS results supported these findings. The unmodified alloy exhibited a high R_{ct} value (13.8 $k\Omega \cdot cm^2$) and restricted Cl^- diffusion (high B and low Y_0), confirming its superior initial corrosion resistance. In contrast, the Sr-modified alloy showed approximately 70.3% lower R_{ct} values, indicating higher initial electrochemical activity. With increasing immersion time, the disappearance of the Warburg diffusion response and the evolution of R_{ct} and R_{oxd} values confirmed the development of a protective corrosion product layer, which enhanced interfacial stability under prolonged exposure conditions.

The corroded surfaces of the unmodified A356 alloy exhibited pronounced α-Al dendrite dissolution together with coarse, plate-like Si particles after both 1 h and 120 h of immersion. In contrast, the Sr-modified alloy exhibited a finer and more homogeneous microstructure. The immersion-time-dependent morphological changes observed by SEM were in good agreement with the electrochemical results and revealed that Sr modification promoted the formation of a finer and more homogeneous microstructure together with a more stable corrosion product layer, thereby improving the long-term corrosion behavior of the A356 alloy.

Overall, although Sr modification reduced the initial corrosion resistance due to increased micro-galvanic activity, it promoted the formation of a more stable and protective surface layer during prolonged immersion. Consequently, Sr modification enhanced the stability of the surface layer and mitigated the propagation of localized corrosion, thereby improving the long-term corrosion behavior of the alloy. These findings indicate that Sr addition may serve as an effective microstructural modification approach for enhancing the long-term durability of Al-Si-Mg alloys exposed to chloride-containing environments.

DECLARATION OF ETHICAL STANDARDS (ETİK STANDARTLARIN BEYANI)

The author of this article declares that the materials and methods they use in their work do not require ethical committee approval and/or legal-specific permission.

Bu makalenin yazarı çalışmalarında kullandıkları materyal ve yöntemlerin etik kurul izni ve/veya yasal-özel bir izin gerektirmediğini beyan ederler.

AUTHORS' CONTRIBUTIONS (YAZARLARIN KATKILARI)

Gökçe HAPÇI AĞAOĞLU: She conducted the experiments, analyzed the results and performed the writing process.

Deneyleri yapmış, sonuçlarını analiz etmiş ve maklenin yazım işlemini gerçekleştirmiştir.

CONFLICT OF INTEREST (ÇIKAR ÇATIŞMASI)

There is no conflict of interest in this study.

Bu çalışmada herhangi bir çıkar çatışması yoktur.

REFERENCES (KAYNAKLAR)

[1] Robles Hernandez, F.C., Herrera Ramírez, J.M., Mackay, R. (2017). Al-Si Alloys: Automotive, Aeronautical, and Aerospace Applications. Springer International Publishing, Switzerland; https://doi.org/10.1007/978-3-319-58380-8.

[2] Ganesh, M.R.S., Reghunath, N., Levin, M.J., Prasad, A., Doondi, S., Shankar, K.V. (2022). Strontium in Al-Si-Mg alloy: A review. Korean Institute of Metals and Materials, 28, 1-40; https://doi.org/10.1007/s12540-021-01054-y.

[3] Berlanga-Labari, C., Biezma-Moraleda, M.V., Rivero, P.J. (2020). Corrosion of cast aluminum alloys: A review. Metals, 10, 1384, 1-30; https://doi.org/10.3390/met10101384.

[4] Cardinale, A.M., Macciò, D., Luciano, G., Canepa, E., Traverso, P. (2017). Thermal and

corrosion behavior of as-cast Al-Si alloys with rare earth elements. Journal of Alloys and Compounds, 695, 2180-2189; https://doi.org/10.1016/j.jallcom.2016.11.066.

[5] Bergmann Kremer, A., Scheidhauer, N., Szucki, M., Keßler, A., Krawczyk, L., Dietrich, I. (2026). Influence of the chemical composition, casting process, grain refinement, and modification on the mechanical and corrosion behaviours of Al-Si casting alloys. International Journal of Metal casting; https://doi.org/10.1007/s40962-025-01861-8.

[6] Arthanari, S., Jang, J.C., Shin, K.S. (2019). Corrosion performance of high pressure die-cast Al-Si-Mg-Zn alloys in 3.5 wt% NaCl solution. Journal of Alloys and Compounds, 783, 494-502; https://doi.org/10.1016/j.jallcom.2018.12.313.

[7] Kim, J., Shin, S., Lee, S. (2022). Correlation between microstructural evolution and corrosion resistance of hypoeutectic Al-Si-Mg alloy: Influence of corrosion product layer. Materials Characterization, 193, 112276; https://doi.org/10.1016/j.matchar.2022.112276.

[8] Ikeuba, A.I., Njoku, C.N., Ekerenam, O.O., Njoku, D.I., Udoh, I.I., Daniel, E.F., Uzoma, P.C., Etim, I.I.N., Okonkwo, B.O. (2024). A review of the electrochemical and galvanic corrosion behavior of important intermetallic compounds in the context of aluminum alloys. RSC Advances, 14, 31921-31953; https://doi.org/10.1039/d4ra06070a.

[9] Arrabal, R., Mingo, B., Pardo, A., Mohedano, M., Matykina, E., Rodríguez, I. (2013). Pitting corrosion of rheocast A356 aluminium alloy in 3.5 wt.% NaCl solution. Corrosion Science, 73, 342-355; https://doi.org/10.1016/j.corsci.2013.04.023.

[10] Osório, W.R., Goulart, P.R., Garcia, A. (2008). Effect of silicon content on microstructure and electrochemical behavior of hypoeutectic Al–Si alloys. Materials Letters, 62, 365-369; https://doi.org/10.1016/j.matlet.2007.05.051.

[11] Osório, W.R., Garcia, L.R., Goulart, P.R., Garcia, A. (2007). Effects of eutectic modification and T4 heat treatment on mechanical properties and corrosion resistance of an Al-9 wt.% Si casting alloy. Materials Chemistry and Physics, 106, 343-349; https://doi.org/10.1016/j.matchemphys.2007.06.011.

[12] Dahle, A.K., Nogita, K., McDonald, S.D., Dinnis, C., Lu, L. (2005). Eutectic modification and microstructure development in Al-Si alloys. Materials Science and Engineering A, 413-414, 243-248; https://doi.org/10.1016/j.msea.2005.09.055.

[13] Tahamtan, S., Boostani, A.F., Nazemi, H. (2009). Pitting corrosion of thixoformed, rheocast and gravity cast A356-T6 alloy in chloride media. Corrosion Engineering Science and Technology, 44, 384-388; https://doi.org/10.1179/174327808X315678.

[14] Pardo, A., Merino, M.C., Merino, S., Viejo, F., Carboneras, M., Arrabal, R. (2005). Influence of reinforcement proportion and matrix composition on pitting corrosion behaviour of cast aluminium matrix composites. Corrosion Science, 47, 1750-1764; https://doi.org/10.1016/j.corsci.2004.08.010.

[15] Olohunde, S.T., Hafizi, A.R.M., Jamaliah, I., Al-Bakoosh, A.A., Segun, O.O., Sadiq, I.O. (2019). Corrosion resistance of aluminium-silicon hypereutectic alloy from scrap metal. Journal of Bio- and Tribo-Corrosion, 5, 41, 1-8; https://doi.org/10.1007/s40735-019-0224-x.

[16] Jie, L.L., Baig, M.F., Mhd Noor, E.E. (2024). Effects of strontium modification on corrosion resistance of Al-Si alloys in various corrosive environments. Materials, 17, 4923, 1-19; https://doi.org/10.3390/ma17194923.

[17] Dahle, A.K., Nogita, K., Zindel, J.W., McDonald, S.D., Hogan, L.M. (2001). Eutectic nucleation and growth in hypoeutectic Al-Si alloys at different strontium levels. Metallurgical and Materials Transactions A, 32A, 949-960; https://doi.org/10.1007/s11661-001-0352-y.

[18] Campbell, J., Tiryakioğlu, M. (2010). Review of effect of P and Sr on modification and porosity development in Al-Si alloys. Materials Science and Technology, 26, 262-268; https://doi.org/10.1179/174328409X425227.

[19] Meena, L. K., Sinha, A. K., Seshagiri, R., Singh, R. (2022). Effects of strontium addition on corrosion properties of Al-12Si Alloy. In

Recent Trends in Electrochemical Science and Technology: Proceedings of Papers Presented at NSEST-2020 and ECSIRM-2020. Springer, Singapore, 35-52; https://doi.org/10.1007/978-981-16-7554-6.

[20] Lee, S.L., Cheng, Y.C., Chen, W.C., Lee, C.K., Tan, A.H. (2012). Effects of strontium and heat treatment on the wear-corrosion property of Al-7Si-0.3Mg alloy. Materials Chemistry and Physics, 135, 503-509; https://doi.org/10.1016/j.matchemphys.2012.05.015.

[21] Lian, P., Mao, H., Wei, Q., Ma, R., Li, C., Xu, H. (2023). Tailoring the strength and corrosion resistance of Al-7Si: Eutectic Si modification by Sr and Sc. Materials Letters, 348, 134505; https://doi.org/10.1016/j.matlet.2023.134505.

[22] Liao, H., Dong, G., Sun, G. (2007). Investigation on influence of sodium- or strontium-modification on corrosion-resistance of Al-11.7%Si alloy. Journal of Materials Science, 42, 5175-5181; https://doi.org/10.1007/s10853-006-0545-2.

[23] Farahany, S., Ourdjini, A., Bakhsheshi-Rad, H.R. (2016). Microstructure, mechanical properties and corrosion behavior of Al-Si-Cu-Zn-X (X=Bi, Sb, Sr) die cast alloy. Transactions of Nonferrous Metals Society of China, 26, 28-38; https://doi.org/10.1016/S1003-6326(16)64085-2.

[24] Duygun, İ.K., Hapçı Ağaoğlu, G., Dispinar, D., Orhan, G. (2019). Time-dependent corrosion properties of Sr-modified AlSi9 alloy analyzed by electrochemical techniques. Journal of Alloys and Compounds, 803, 786-794; https://doi.org/10.1016/j.jallcom.2019.06.330.

[25] Öztürk, İ., Hapçı Ağaoğlu, G., Erzi, E., Dispinar, D., Orhan, G. (2018). Effects of strontium addition on the microstructure and corrosion behavior of A356 aluminum alloy. Journal of Alloys and Compounds, 763, 384-391; https://doi.org/10.1016/j.jallcom.2018.05.341.

[26] McCafferty, E. (2003). Sequence of steps in the pitting of aluminum by chloride ions. Corrosion Science, 45, 1421-1438; https://doi.org/10.1016/S0010-938X(02)00231-7.

[27] Ahmad, Z. (1986). The kinetics of anodic and cathodic polarization of aluminium and its alloys. Anti-Corrosion Methods and Materials, 33, 4-11; https://doi.org/10.1108/eb020492.

[28] Zhou, W., Xue, F., Li, M. (2025). Corrosion behavior of Al-Mg alloys with different alloying element contents in 3.5% NaCl solution. Metals, 15, 327; https://doi.org/10.3390/met15030327.

[29] Duygun, I.K., Agaoglu, G.H., Orhan, G. (2020). Investigation of time-dependent corrosion behavior of Sr-modified AlSi12 alloy. International Journal of Materials Research, 111, 339-346; https://doi.org/10.3139/146.111882.

[30] Moreto, J.A., Marino, C.E.B., Bose Filho, W.W., Rocha, L.A., Fernandes, J.C.S. (2014). SVET, SKP and EIS study of the corrosion behaviour of high strength Al and Al-Li alloys used in aircraft fabrication. Corrosion Science, 84, 30-41; https://doi.org/10.1016/j.corsci.2014.03.001.